

AD-A083 680

CATHOLIC UNIV OF AMERICA WASHINGTON DC DEPT OF PHYSICS
RESONANCES OF RADAR TARGETS AND TARGET DISCRIMINATION.(U)
MAR 80 H UBERALL

F/8 17/9

NO0019-79-C-0270

ML

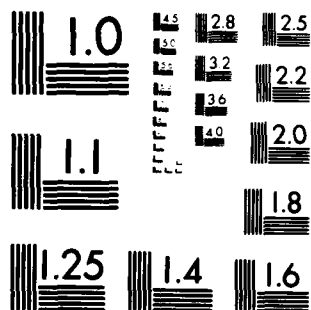
UNCLASSIFIED

(U)

SECRET



END
DATE
FILMED
6-80
DTIC



MICROCOPY RESOLUTION TEST CHART
NATIONAL BUREAU OF STANDARDS-1963-A

ADA 083680

Final Report
6 Mar 79 - 5 Mar 80 NW

Resonances of Radar Targets and Target Discrimination

Naval Air Systems Command
Contract No. N00019-79-C-0270

Reporting Period
March 6, 1979 to March 5, 1980

MARCH 1980

Prepared by:

Herbert Uberall Principal Investigator
Department of Physics
Catholic University
Washington, DC 20064

| | | |
|--------------------|-----------------------|---|
| Accession For | | A |
| NTIS Serial | | |
| DDC TAB | | |
| Unannounced | | |
| Justification | | |
| By | | |
| Distribution / | | |
| Availability Codes | | |
| Dist | Available for special | |

APPROVED FOR PUBLIC RELEASE
DISTRIBUTION UNLIMITED


80 4 28 127

I. Introduction

This is the final report on the research program "Resonances of Radar Targets and Target Discrimination", supported by the Naval Air Systems Command under Contract No. N00019-79-C-0270, and covering the period March 6, 1979 to March 5, 1980.

The topic of the research program covers methods for target discrimination by radar scattering, making use of the natural resonances of the targets. The general plan of the program consists in a study of resonances of targets of simple shape (e.g., sphere) but complex composition (e.g., dielectric coating of conductors) during the first year, followed by simple conducting targets and comparison with parallel measurements performed at NSWC Dahlgren in the second year, with further extension to conductors of more complex shapes, using Waterman's methods, later on.

The emphasis of our study is two-fold, namely: 1) to study ways how the resonance structure of the radar echo can be used for identifying the nature of the target (the "inverse scattering problem") and 2) to obtain a physical understanding of the phenomena that cause the resonances, and how they manifest themselves in both steady-state and pulsed echoes. Such an understanding, in preference to a more mechanical use of the singularity expansion method, will provide us with the true capability of mastering the target discrimination problem.



II. Progress Achieved

The first year's research has concerned steady-state studies of the resonances of dielectric spheres and dielectric-coated conducting spheres. In the following, superscripts refer to the list of publications which were prepared under the auspices of this contract, and which are listed in Section III.

1) Dielectric Sphere¹. The Theory of Resonance Scattering² developed by the Principal Investigator and his collaborators has been applied to this problem in order to

(a) obtain resonance frequencies (as a function of dielectric constant) in a purely real calculation, in contrast to previous tedious solutions of the complex problem

(b) interpret the resonances physically in terms of the phase matching of circumferential waves, and

(c) obtain the properties (in particular, the dispersion curves) of these circumferential waves.

This work has been submitted for publication in IEEE Trans. AP¹ and has been reported³ at the National Radio Science Meeting, 5-8 November 1979, Boulder, Colorado.

2) Dielectric-Coated Perfectly Conducting Sphere. This problem has been approached from the stand point of inverse scattering, in order to show how the dielectric constant and the thickness of the coating can be obtained from the spacing and the widths of the resonances⁴⁻⁷. A complete resonance-theoretical treatment has been performed on this topic^{8,9}, separating the scattering amplitudes

into resonant terms and a non-resonant background, and obtaining the dispersion curves of the circumferential waves that propagate in the coating and cause the resonances⁹.

Our work on this problem has been prepared for publication in Journ. Appl. Phys⁴, and other aspects of it in Radio Science⁹, and it will be reported at the North American Radio Science/URSI meeting, 2-6 June, 1980, Quebec, Canada⁵, (abstract attached) as well as the Spring Meeting of the American Physical Society, 28 April-1 May, Washington, D. C. (abstract attached). It will further form part of an Invited Paper for a Special Issue on "Inverse Methods in Electromagnetics" (W. M. Boerner, Editor), IEEE Trans. A-P, Spring 1981. A copy of this latter paper is attached to the present report.

3) The Transient Problem of Conducting Bodies.

A collaboration with an experimental group at the Naval Surface Weapons Center, Dahlgren, VA led by Dr. Bruce Hollmann has been initiated, with pulsed measurements to be carried out at the Dahlgren radar range on conducting bodies of simple shapes, to be compared to theory (both the Singularity Expansion Method or SEM, and Creeping Wave Theory). Meanwhile, we obtained the theory for an experiment on a conducting sphere, and have established the connection between SEM and Creeping-Wave theory, with the latter providing physical insight into the SEM results. Our analytical results are now being programed, and will be published for acoustic¹⁰ as well as radar targets¹¹ of spherical

shape in the near future. Similar studies are now being undertaken by A. Nagl and F. Cannata for conducting infinite or finite cylinders.

III. Personnel

The following personnel has been involved in the work described in the present progress report:

H. Uberall, Professor, Catholic University, Principal Investigator

A. Nagl, Catholic University, Research Associate

P. J. Moser, Catholic University, Graduate Student (also Naval Research Laboratory, Washington, D. C.)

F. Cannata, Catholic University, temporary Research Associate

J. D. Murphy, Annandale, VA, voluntary collaborator

L. Flax, Naval Research Laboratory, Washington, D. C.

G. C. Gaunard, Naval Surface Weapons Center, White Oak, Silver Spring, MD

L. R. Dragonette, Naval Research Laboratory, Washington, D. C.

J. Severns, Naval Research Laboratory, Washington, D. C.

III Publications and Abstracts of Talks Supported or Partly
Supported by Present Contract.

1. J. D. Murphy, P. J. Moser, A. Nagl, and H. Uberall, "A Surface Wave Interpretation for the Resonances of a Dielectric Sphere", IEEE Trans. AP (accepted for publication)
2. L. Flax, G. C. Gaunaurd, and H. Uberall, "Theory of Resonance Scattering", Physical Acoustics Vol. 15, Academic Press, New York, 1980 (in press).
3. J. D. Murphy, P. J. Moser, A. Nagl, and H. Uberall, "A Surface Wave Interpretation for the Resonances of a Dielectric Sphere", paper B4-3, International Union of Radio Science, National Radio Science Meeting, 5-8 November 1979, Boulder, Colorado.
4. G. Gaunaurd, H. Uberall, and P. J. Moser, "Resonances of Dielectrically-Coated Conducting Spheres and the Inverse Scattering Problem", to be published in Journal of Appl. Phys.
5. P. J. Moser, J. D. Murphy, A. Nagl, H. Uberall, and G. C. Gaunaurd, "Resonances of a Dielectrically Coated Conducting Sphere: Surface Waves and the Inverse Scattering Problem", paper submitted to the North American Radio Science Meeting (URSI, Commission B), Quebec, Canada, 2-6 June, 1980.
6. G. C. Gaunaurd and H. Uberall, "Solution of Inverse Scattering Problems in the Resonance Case", paper submitted to the Washington Meeting of the American Physical Society, 28 April - 1 May, 1980.
7. G. Gaunaurd, H. Uberall, and L. R. Dragonette, "Solution of the Inverse Electromagnetic, Acoustic, and Elastic Scattering Problem in the Resonance Case", Invited paper for the IEEE Transactions AP, Special issue on "Inverse Methods in Electromagnetics" (W.M.Boerner Editor), Spring 1981.

8. J. D. Murphy, A. Nagl, and H. Uberall, "Resonance Effects in Radar Scattering from Conducting Dielectric, and Coated Targets", Navair Electronic Research Program Review, Stanford, University, Stanford, CA, 6 March, 1979.
9. P. J. Moser, J. D. Murphy, and H. Uberall, "Resonances and Surface Waves in Conducting Spheres with Dielectric Coating", Radio Science (to be published).
10. H. Uberall, and J. D. Murphy, "Acoustic Surface Wave Pulses and the Ringing of Resonances", J. Acoust. Soc. Am. (to be prepared for publication).
11. H. Uberall and J. D. Murphy, "The Physical Content of the Singularity Expansion Method", IEEE Trans. A-P (to be prepared for publication).

(CONFIDENTIAL)
2-0, 1-0
NORTH AMERICAN RADIO SCIENCE MEETING
and
IEEE/APS INTERNATIONAL SYMPOSIUM

Université Laval, Cité universitaire
Québec, Canada

RESONANCES OF A DIELECTRICALLY COATED CONDUCTING SPHERE:
SURFACE WAVES AND THE INVERSE SCATTERING PROBLEM.

Philip J. Moser, J. Diarmuid Murphy, Anton Nagl, and
Herbert Überall

Department of Physics, Catholic University
Washington, DC 20064

Guillermo C. Gaunard, Naval Surface Weapons Center
White Oak, Silver Spring, MD 20910

The theory of resonance scattering, developed by some of the present authors in the context of the scattering of acoustic waves from elastic obstacles, or of elastic waves from fluid-filled cavities or solid inclusions, is here applied to the problem of radar scattering from dielectrically-coated, perfectly conducting spherical targets. The numerous, sharp and narrow resonances obtained in previous calculations of the corresponding radar cross sections (see, e.g., Ruck et al, Radar Cross Section Handbook, Plenum New York, 1970) are shown here to correspond to the real resonance frequencies of the target, which can be calculated from a real characteristic equation and agree approximately with the real part of the natural frequencies. A surface-wave interpretation of these resonances is made entirely on the basis of real analysis, thus avoiding the complexities of the Watson transformation. The dispersion curves for these surface waves are obtained, which show (for the TM mode) a discontinuous transition from conductor-type at low frequencies to dielectric-type at high frequencies. The inverse problem is also solved (see, e.g., G. C. Gaunard, H. Überall, and L. R. Dragonette, IEEE Trans. Antennas Propag., Special Issue on Inverse Methods in Electromagnetics, W. M. Boerner, ed., to be published) by showing how from the spacing and the widths of the resonances, the dielectric constant and the thickness of the coating may be obtained. Finally, the relationship between the present resonance theory, and the singularity expansion method or SEM (see, C. E. Baum, Interaction Note 88, December 1971) is briefly sketched.

Commission B

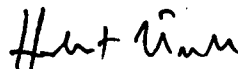
Abstract Submitted
for the Washington Meeting of the
American Physical Society
21-24 April, 1980

Physics and Astronomy
Classification Scheme
Number 41.10.Hv

Suggested title of session
in which paper should be placed
Mathematical Physics; General
Interest.

Solution of Inverse Scattering Problems
in the Resonance Case. G. C. Gaunard and
H. Überall, Naval Surface Weapons Center,
White Oak, Silver Spring, MD 20910. We show
that whenever resonances are present in the
echoes of electromagnetic, acoustic or elastic
waves scattered from corresponding targets, the
"Theory of Resonance Scattering" recently
developed by us¹ leads to a simple and direct
solution of the inverse scattering problem. We
have found in all three cases that the spacing
between consecutive resonances, and their
widths, contain the information needed for a
determination of the material parameters of the
scatterer, and in the case of coated targets, of
the coating thickness. This constitutes a
straightforward answer to the inverse scattering
problem via the resonance formalism. (H. Überall
is also at Catholic University, Washington, DC,
additionally supported by NAVAIR Code AIR-310-B)
1. L. Flax, G. C. Gaunard, and H. Überall, "Reso-
nance Theory of Scattering", Physical Acoustics 18.

(✓) Prefer Standard Session


Signature of APS Member

Herbert Überall
Same Name Typewritten
Physics Department
Catholic University
Address
Washington, DC 20064

SOLUTION OF THE INVERSE ELECTROMAGNETIC, ACOUSTIC, AND ELASTIC
SCATTERING PROBLEM IN THE RESONANCE CASE.

G. Gaunaurd and H. Überall*

Naval Surface Weapons Center
White Oak, Silver Spring, MD 20910

and

L. R. Dragonette
Naval Research Laboratory
Washington, DC 20375

* Also at the Department of Physics, Catholic University,
Washington, DC 20064

Abstract

Conventional methods of attacking the inverse scattering problem are either based on the geometrical optics limit, or on the use of Fredholm integral equations of the first kind. We demonstrate here that for the (quite common) case that resonances are present in the echoes of electromagnetic, acoustic or elastic waves scattered from corresponding targets, the theory of resonance scattering recently developed by us represents a powerful tool for the solution of the inverse scattering problem. For example, for the case of elastic-wave scattering from fluid-filled spherical cavities in solids, the spacing of successive resonances determines the sound speed of the fluid-filler, and the resonance widths its density. Measurements of the resonances were performed by us for acoustic scattering from submerged elastic objects. For the case of electromagnetic scattering from dielectric or coated conducting targets, spacing and widths of the resonances are shown to determine the dielectric constant and the coating thickness of the target object in a direct fashion.

I. Introduction

Inverse scattering is of importance in many fields of Physics. In quantum mechanics, inverse scattering methods try to determine the potential if the scattering cross section is known. Geophysicists attempt to determine the distribution of density and of seismic velocity with depth, from observed reflection responses. In general, inverse scattering methods try to obtain information about a source distribution, a scattering obstacle or inhomogeneity of a medium from remotely-sensed field data.

Attempts at a solution of the inverse scattering problem have conventionally proceeded via the use of the geometrical-optics limit, or else via an exact treatment that leads to Fredholm integral equations of the first kind¹. In the present review, we wish to demonstrate that if resonances are present in the scattering cross sections as a function of frequency, then the measurable characteristics of these resonances furnish us with a powerful tool for the solution of the inverse scattering problem, i.e. for the determination of the geometry and the composition of the target from the measured properties of the echo returns. In fact, the presence of resonances in scattering echoes seems to be the rule rather than the exception, as confirmed for the cases of acoustic² and elastic-wave³, as well as electromagnetic⁴ scattering.

The theory of resonance scattering, as developed by us recently⁵⁻⁸, provides a formalism that may be used for a straightforward and direct solution of the inverse scattering problem.

Although this will be demonstrated in the following on the basis of a few simple examples only (reflection of acoustic waves from plane layers; of elastic waves from fluid-filled spherical cavities; and of electromagnetic waves from dielectrically-coated conducting spheres), it is clear that an elaboration of these procedures for the case of more complex targets will, with proper attention to detail, provide us with a wealth of information on both the geometry and the composition of the target which hitherto seems to have been largely disregarded.⁹ Our examples show that, e.g., the spacing of successive resonances in elastic-wave echoes directly determines the sound speed in the fluid filler of a spherical cavity, and that the resonance widths determine the density of the fluid; or that for the case of electromagnetic scattering from spherical dielectric or coated conducting targets, the spacing and widths of the resonances determine the dielectric constant and the coating thickness of the target object in a direct fashion. The resonances thus characterize the scattering object as if they were its signature, and their spectrum constitutes a code identifying the target in a way that resembles optical spectroscopy.

II. Acoustic Resonances

The first example to be discussed is the acoustic transmission and reflection for a plane fluid¹⁰ or elastic¹¹ layer of thickness d imbedded in an ambient fluid. The latter will be characterized by its density ρ and sound velocity c , while the (elastic) layer is assumed to have density ρ_d , and compressional and shear speeds c_d and c_t , respectively. A plane sound wave be incident at an

angle θ with the normal, and be refracted at angles α for compressional, or β for shear waves into the layer. The transmission (T) and reflection coefficients (R) may be written in the form

$$T = i\tau \left(\frac{1}{C_s - i\tau} + \frac{1}{C_a + i\tau} \right), \quad (1a)$$

$$R = \frac{C_s C_a - \tau^2}{C_s + C_a} \left(\frac{1}{C_s - i\tau} + \frac{1}{C_a + i\tau} \right) \quad (1b)$$

where

$$\tau = \frac{\rho c / \cos \theta}{\rho_d c_d / \cos \alpha} = \frac{\rho}{\rho_d} \frac{(n_d^2 - \sin^2 \theta)^{1/2}}{\cos \theta}, \quad (1c)$$

$$n_d = c / c_d, \quad n_t = c / c_t. \quad (1d)$$

For a lossless layer, one has $|T|^2 + |R|^2 = 1$. The ("symmetric", s, and "antisymmetric", a) coefficients C_s and C_a are given in the literature¹¹; for a fluid layer ($c_t \rightarrow 0, \beta \rightarrow 0$), one finds

$$C_s \rightarrow \cot \delta, \quad C_a \rightarrow \tan \delta \quad (2a)$$

where

$$\delta = \frac{kd}{2} (n_d^2 - \sin^2 \theta)^{1/2} = \frac{x}{2} (n_d^2 - y^2)^{1/2}, \quad (2b)$$

using the abbreviations $x = kd = \omega d/c$, $y = \sin \theta$. If $n_d < n_t < 1$, the critical angles of total reflection

$$\theta_d = \sin^{-1} n_d, \quad \theta_t = \sin^{-1} n_t \quad (2c)$$

appear.

Equations (1a, b) show that each of the two terms in T as well as in R will exhibit a resonance behavior when the real parts of the denominators vanish:

$$C_s = 0 \quad \text{or} \quad C_a = 0 \quad (3a)$$

These equations also describe the free-plate dispersion relations^{10,11} (corresponding to no fluid-loading, $\tau \rightarrow 0$) for the characteristic waves on the plate. The resonances will be the more pronounced, the smaller the imaginary part τ of the denominator (roughly speaking, $\rho_c/\rho_d C_d \ll 1$), i.e. the lighter the fluid loading. For the fluid layer, Eqs. (3a) have the solutions

$$\cot \delta = 0, \quad \delta = \delta_{m_s} = (m_s + \frac{1}{2})\pi \quad (3b)$$

or

$$\tan \delta = 0, \quad \delta = \delta_{m_a} = m_a \pi, \quad (3c)$$

with m_s and m_a being integers.

The two independent variables of the problem may be taken as x and y . Resonance forms of T and R may be obtained in either of these variables, holding the other one fixed.

Taking y fixed, we expand the functions C_s or C_a around their resonance values:

$$C_{s,a}(x) \approx (x - x_{m_s,a}) C_{s,ax}(x_{m_s,a}), \quad (4)$$

where $x_{m_s,a}$ designate the solutions of $C_{s,a}(x) = 0$, and $C_{s,ax} = \partial C_{s,a} / \partial x$. For the reflection coefficient, e.g., this leads to the resonance form

$$T = \sum_{m_s} \frac{-\frac{1}{2} i \Gamma_{m_s}}{x - x_{m_s} + \frac{1}{2} i \Gamma_{m_s}} + \sum_{m_a} \frac{\frac{1}{2} i \Gamma_{m_a}}{x - x_{m_a} + \frac{1}{2} i \Gamma_{m_a}}, \quad (5a)$$

with each resonance expression being valid in the vicinity of its own resonance position $x = x_{ms,a}$. For the elastic plate, Eqs. (3a) have to be solved numerically for $x_{ms,a}$, for the fluid plate, one has

$$x_{ms,a} = 2 \int_{m_{s,a}} (n_d^2 - \sin^2 \theta)^{-1/2}. \quad (5b)$$

The resonance widths are

$$\Gamma_{m_{s,a}} = \mp 2\tau / C_{s,a} x(x_{ms,a}), \quad (5c)$$

which for the fluid plate become independent of $m_{s,a}$:

$$\Gamma = 4\eta / (\rho_d \cos \theta). \quad (5d)$$

These resonances may be interpreted as poles in the lower half of the complex x -plane, located at

$$x_{pole} = x_{ms,a} - \frac{1}{2} i \Gamma_{m_{s,a}}. \quad (5e)$$

Similar resonance expressions may be derived for R , as well as for T and R as functions of the y - variable.

Equation (5a) is illustrated in Fig. 1 for a water layer in alcohol, at various values of θ . Figure 2 illustrates resonances in the angular variable of the transmission loss $TL \equiv \log |T|^2$ for a steel plate in water. The figures show both the results for the individual resonance terms, Eq. (5a), and as obtained from the exact expression, Eq. (1a). The value of the resonance formalism lies in the fact that it furnishes explicit expressions for the position, width, and strength of each resonance contribution, Eqs. (5b)-(5d), as a function of all the material parameters.

It thus appears possible to carry out an inverse determination of the material constants of a plate by examining the resonances experimentally. In fact, for a fluid layer, Eqs. (5b) and (3b,c) show that the resonance positions measure, via $n_d = c/c_d$, the sound speed c_d in the layer, and Eq. (5d) shows that the width of the resonances measures the density ratio ρ/ρ_d . This is the simplest example for the solution of the inverse scattering problem via a study of the resonances. For the elastic plate, the inverse-scattering solution proceeds analogously and is only slightly more involved. While for the fluid layer, Eq. (5b) is physically understood by the kinematic condition that the normal component of the layer wave number equals $k_d = m\pi/d$, corresponding to an integer number of half-wavelengths across the layer, this picture is no longer true for elastic layers where shear waves enter also. Here, the physical understanding is provided by the coincidence of the trace velocity of the incident wave with the speed of the characteristic

waves propagating along the free plate¹¹. However, Eqs. (5c) or (5d) which complete the inverse problem, are only obtained from a dynamic calculation.

III Elastic Wave Resonances

In this section, we shall discuss an application of the Resonance Theory of (visco)elastic wave-scattering that solves an inverse scattering problem of elastodynamics. The procedure, like that discussed in the preceding section, sets the pace for extensions to more general situations, as well as for direct transfer to other neighboring scientific areas.

The amplitudes of backscattered waves returned by obstacles in viscoelastic solids³, when plotted as a function of frequency, exhibit so many rapid oscillations and complicated features that until very recently it was not possible to extract the physical information contained in them about the nature of the obstacle. We can analyze these backscattered "echoes" using the Resonance Theory of viscoelastic wave-scattering from cavities in solids, and obtain from them, for a given shape of the cavity, the material composition of the filler substance (assumed fluid in this example, for simplicity).

When a (spherical) cavity filler is sent into oscillation by elastic (say, compressional, or p-type) incident waves, a set of modal resonances (fundamental and overtones) are excited in it, that characterize the filler as if it were its signature. The way these resonances can be used for material discrimination purposes resembles

the way chemical elements are identified from their optical spectra.

The far-field backscattering amplitude of p-waves, returned by a spherical fluid-filled cavity of radius a in a solid under p-wave incidence, is given⁷ by the "partial wave sum"

$$\frac{1}{a} f_{\infty}^{pp}(\pi) = \sum_{n=0}^{\infty} \frac{1}{a} f_n^{pp}(\pi) = \sum_{n=0}^{\infty} (-1)^n \frac{2n+1}{2i\kappa_d a} (S_n^{pp} - 1) \quad (6)$$

where $\kappa_d = k_d (1 - i\omega M)^{1/2}$ ($k_d = \omega/c_d$, c_d = p-wave velocity) is the compressional wave number in the ambient solid, which is complex if the solid is viscoelastic ($M \neq 0$). The S-matrix element S_n^{pp} is given in the literature⁷. Figure 3 shows the plot of the modulus of the summed amplitude in the backscattering direction $\theta = \pi$ (i.e., $|f^{pp}(\pi)/a|$) for a cavity filled with ethyl-alcohol in an aluminum matrix. This is the "echo" containing the rapid oscillations and complex features mentioned above. Fifteen partial waves were added to produce that plot, which for the range $0 \leq k_d a \leq 10$ of Fig. 3, yields enough accuracy. This is the amplitude as a sensor would record it.

An analysis of the first partial-wave contributions making up the sum is shown in Fig. 4. Each mode can be split into a background (center graph) and resonances (bottom graph). An index ℓ labels each resonance of each mode n . Overlaying the resonances which we just isolated, on top of the summed amplitude of Fig. 3, identifies each extremum in that plot with the sets of modal reso-

nances contained in the partial waves. The resonance responsible for each wiggle of Fig. 3 is labeled by indices (n, ℓ) , and the graph shows over thirty wiggles uniquely identified with modal resonances in this fashion. The location of all the resonance spikes in fact identifies the ratio c_f/c_d of the filler-to-matrix wavespeeds. The filler's sound-speed c_f can be found from the spacing Δ between any two high-order consecutive overtones shown in Fig. 4. For spherical cavities in solids, we have shown¹²⁻¹⁴ that for $\ell \gg 1$, one obtains

$$\Delta \cong \pi (c_f / c_d). \quad (7)$$

For alcohol in aluminum, that relation gives $\Delta \cong 0.59$, just as observed in Fig. 4. Thus, knowing c_d for the matrix, and the spacing Δ between consecutive high-order modal resonances, determines the sound speed c_f of the filler, and vice versa.

As in the acoustic case, the resonance theory of scattering leads to a resonance form of the scattering amplitude^{7,12}:

$$\begin{aligned} \frac{1}{\alpha} f_n^{pp}(\pi) = & (-1)^n \frac{2n+1}{2i\kappa_d a} e^{2i\xi_n} \left[\sum_{\ell=1}^{\infty} \frac{M_{n\ell}}{X - X_{n\ell} + \frac{i}{2}\Gamma_{n\ell}} \right. \\ & \left. + 2i \exp(-i\xi_n) \sin \xi_n \right], \end{aligned} \quad (8)$$

where $S_n^{(0)pp} \equiv \exp(2i\xi_n)$ represents the S-matrix element of a "soft" (i.e., evacuated) cavity. The first term in brackets of Eq. (8) leads to the resonances (bottom portion of Fig. 4), and the second term to the non-resonant background (center portion of Fig. 4); their coherent addition produces the interference effects in each partial wave (top portion of Fig. 4). The resonance frequencies x_{nl} refer to a normalized frequency scale $x = k_d a$.

The density ratio of filler-to-matrix materials (i.e., ρ/ρ_f) is found from the resonance widths. Explicit forms for the widths Γ_{nl} of the resonances may be given^{7, 12-14}, and were shown to depend on ρ/ρ_f , via the mechanical impedance $F_n(x)$ of the obstacle which is a known quantity. If we evaluate the latter at a point one half-width below any resonance peak (i.e., $x = x_{nl} - \Gamma_{nl}/2$) and then expand for $x \gg 1$, the result is

$$\frac{\rho_f}{\rho} \xrightarrow{x \gg 1} -\frac{1}{(\ell + \frac{n}{2} - \frac{1}{2})\Delta} + \frac{\pi^2}{\Delta^2} \frac{\Gamma_{nl}}{2} + \dots, \quad (9)$$

$$(n, \ell = \text{integers}),$$

which holds for integer n and $\Gamma_{nl} < 2\Delta$, so that consecutive resonances do not overlap. In the high-frequency limit, this gives the filler-to-matrix density ratio in terms of the uniform asymptotic spacing Δ , and the width Γ_{nl} of any (high-index) overtone ℓ , of any mode n , which are either all known or previously determined quantities.

For ethyl alcohol ($\rho_f = 0.79 \text{ g/cm}^3$, $c_f = 1.213 \times 10^5 \text{ cm/sec}$) in aluminum ($\rho = 2.7 \text{ g/cm}^3$, $c_d = 6.420 \times 10^5 \text{ cm/sec}$) we find $\Delta \cong 0.59$, and for the first (i.e., $n = 1$) mode, the graphical width of its tenth overtone ($l = 10$), which occurs at $x_{nl} \cong l\Delta = 5.93$, is approximately 0.06, as found from a plot similar to the bottom portion of Fig. 4. To obtain the width Γ_{nl} as defined in Eq. (8), we must still¹² divide by $\sqrt{3}$, and substitution into Eq. (9) yields $\rho_f / \rho = 0.296$, which contains a negligible error when compared to the true ratio $0.79/2.70$. The (fluid) filler is completely identified once its sound speed and density are determined by this asymptotic procedure. We conclude that the sound-speed ratio between filler and matrix is extracted from the spacing between any two consecutive overtones of any mode, and the matrix-to-filler density ratio is extracted from the width of any high-order resonance by means of Eq. (9). Thus, the high-frequency region $x \gg 1$, $l \gg 1$ contains all the information about the material composition of the filler. The filler has been identified from its "echo", and an inverse scattering problem has been solved in a novel fashion.

Echo spectra from fluid filled cavities, such as that shown in Fig. 3, have been measured by Pao and Sachse³ using ultrasonic techniques. In acoustics, measurements of echoes from submerged elastic objects have been performed using short-pulse experimental techniques². Figure 5 shows the (total) far-field scattering amplitude modulus for an aluminum cylinder in water, plotted vs. ka where $k = \omega/c$ is the wave number of sound in water, and a the cylinder radius. The measured points agree well with an exact

calculation (solid curve), demonstrating the accuracy with which the interference minima caused by the resonances may be experimentally determined in the acoustic case, and hence the accuracy with which the inverse problem may be solved here.

IV Electromagnetic Wave Resonances

A procedure analogous to the one used above for elastic-wave scattering will now be employed in order to solve the inverse scattering problem for electromagnetic waves from a dielectrically coated, perfectly conducting sphere. For a plane wave with propagation constant $k = \omega/c$ incident along the z-axis on the coated sphere, the far-field amplitude of the scattered electric field is given by⁴

$$\vec{E}_{sc} = E_0 \frac{e^{ikr}}{r} \left[\hat{e}_\theta S_1(\theta) \cos \phi - \hat{e}_\phi S_2(\theta) \sin \phi \right], \quad (10)$$

using spherical coordinates, and designating

$$S_1(\theta) = -i \sum_{n=1}^{\infty} (-1)^n \frac{2n+1}{n(n+1)} \left[a_n \frac{P_n^1(\cos \theta)}{\sin \theta} - b_n \frac{dP_n^1(\cos \theta)}{d\theta} \right], \quad (11a)$$

$$S_2(\theta) = -i \sum_{n=1}^{\infty} (-1)^n \frac{2n+1}{n(n+1)} \left[a_n \frac{dP_n^1(\cos \theta)}{d\theta} - b_n \frac{P_n^1(\cos \theta)}{\sin \theta} \right]. \quad (11b)$$

The "Mie coefficients" are given by

$$a_n = - \frac{x j_n(x) - i Z_n (x j_n(x))'}{x h_n^{(1)}(x) - i Z_n (x h_n^{(1)}(x))'} \quad , \quad (12a)$$

$$b_n = - \frac{x j_n(x) - i Y_n (x j_n(x))'}{x h_n^{(1)}(x) - i Y_n (x h_n^{(1)}(x))'} \quad , \quad (12b)$$

where $x = ka$, a being the (outer) radius of the spherical target. For a perfectly conducting sphere, the modal impedances and admittances Z_n and Y_n , respectively, become $Z_n \rightarrow 0$ and $Y_n \rightarrow \infty$. For a coated conducting sphere (radius b of the conducting core, thickness $d = a - b$) which will be considered below, expressions for Z_n and Y_n are given in the literature⁴.

The eigenvibrations of the target correspond to the zeroes of the denominators of a_n and b_n . The resulting characteristic equations

$$1/i Z_n = (x h_n^{(1)}(x))' / (x h_n^{(1)}(x)), \quad (\text{TE modes}) \quad (13a)$$

$$i Y_n = x h_n^{(1)}(x) / (x h_n^{(1)}(x))' \quad (\text{TM modes}) \quad (13b)$$

lead to complex eigenfrequencies. However, since the resonances of the problem are sharp and narrow (as seen from the following figures), indicating small imaginary parts of the denominators, it is sufficient to search for the zeroes of the real parts of the denominators. The corresponding equations

$$1/iZ_n = \text{Re}\{ (x h_n^{(1)}(x))' / (x h_n^{(1)}(x)) \}, \quad (\text{TE modes}) \quad (14a)$$

$$iY_n = \text{Re}\{ (x h_n^{(1)}(x)) / (x h_n^{(1)}(x))' \} \quad (\text{TM modes}) \quad (14b)$$

are solved by the real eigenfrequencies $x = x_{ml}^{\text{TE}}$ and x_{ml}^{TM} of the TE and TM modes, respectively.

Our resonance theory may again be applied to the present scattering problem¹⁵, by writing the Mie coefficients in the form

$$a_n = \frac{1}{2} e^{2i\xi_n^{\text{TE}}} \left\{ \frac{(\tilde{z}_n^{(1)})^{-1} - (\tilde{z}_n^{(2)})^{-1}}{(iZ_n)^{-1} - (\tilde{z}_n^{(1)})^{-1}} + 2i e^{-i\xi_n^{\text{TE}}} \sin \xi_n^{\text{TE}} \right\}, \quad (15a)$$

$$b_n = \frac{1}{2} e^{2i\xi_n^{\text{TM}}} \left\{ \frac{\tilde{z}_n^{(1)} - \tilde{z}_n^{(2)}}{iY_n - \tilde{z}_n^{(1)}} + 2i e^{-i\xi_n^{\text{TM}}} \sin \xi_n^{\text{TM}} \right\}, \quad (15b)$$

where

$$Z_n^{(i)} = \frac{x h_n^{(i)}(x)}{(x h_n^{(i)}(x))'} \quad (i=1,2) \quad (16)$$

and where we designated

$$-\frac{h_n^{(2)}(x)}{h_n^{(1)}(x)} = e^{2i\xi_n^{TE}}, \quad (17a)$$

$$-\frac{(x h_n^{(2)}(x))'}{(x h_n^{(1)}(x))'} = e^{2i\xi_n^{TM}}, \quad (17b)$$

these latter expressions representing the scattering amplitudes from a conducting sphere. While thus the second terms in brackets of Eqs. (15) will provide a non-resonant background to the scattering amplitudes, the first terms provide resonances as in the previous sections. In fact, expanding their denominators about the resonance frequencies x_{nl}^{TE} and x_{nl}^{TM} , one may bring the Mie coefficients into the form

$$a_n = \frac{1}{2} e^{2i\xi_n^{TE}} \left\{ \sum_{l=1}^{\infty} \frac{M_n^{TE}}{X - X_{nl}^{TE} + \frac{i}{2} \Gamma_{nl}^{TE}} + 2i e^{-i\xi_n^{TE}} \sin \xi_n^{TE} \right\}, \quad (18a)$$

$$b_n = \frac{1}{2} e^{2i\xi_n^{TM}} \left\{ \sum_{l=1}^{\infty} \frac{M_n^{TM}}{X - X_{nl}^{TM} + \frac{i}{2} \Gamma_{nl}^{TM}} + 2i e^{-i\xi_n^{TM}} \sin \xi_n^{TM} \right\}, \quad (18b)$$

exhibiting the resonances directly. From the mentioned expansions, explicit expressions for the widths Γ_{nl}^{TE} , Γ_{nl}^{TM} may also be obtained¹⁵.

The electromagnetic resonances are illustrated in Fig. 6 for the example of a perfectly conducting sphere, coated with a dielectric of relative coating thickness $\delta_r = \delta/a = 0.1$, and dielectric constant $\epsilon_1 = 6$. The backscattering cross section⁴,

$$\sigma = \frac{4\pi}{k^2} \left| \sum_{n=1}^{\infty} (-1)^n (n + \frac{1}{2}) (a_n - b_n) \right|^2, \quad (18c)$$

is plotted vs. ka up to 25. Numerous resonances are visible here, and have been identified as TE or TM resonances by solving Eqs. (14a) or (14b). These solutions, denoted by $(nE\ell)$ or $(nM\ell)$, respectively, are marked by arrows in Fig. 6, thus indicating how the resonances may be read off a measured backscattering cross section curve obtained as function of frequency, in order to carry out an inverse scattering analysis. In fact, Fig. 6 may be viewed

as the "characteristic spectrum" identifying the scattering object.

We have also evaluated numerically some of the partial wave coefficients a_n and b_n which exhibit the $(n\pi/\ell)$ and $(n\pi/\ell)$ resonances for a given partial wave number n . Figure 7 presents the TE moduli $[(2n+1)/n(n+1)]|a_n|$ for $n = 9$ (top) and 10 (bottom) plotted vs. ka . The fundamental ($\ell = 1$) partial wave resonance is clearly visible on the left of each figure, while the remaining broad structures are dominated by the conducting-sphere background [second term in square brackets of Eqs. (18)], in which the overtone ($\ell \geq 2$) resonances (first term in square brackets) are imbedded. The separation of these resonances from the background will be described in a forthcoming paper¹⁶.

Using the expressions of Eqs. (18), and the known forms of Z_n and Y_n , the inverse problem may now be solved as in the previous cases. For the higher-order resonances located in the high-frequency spectral region ($x \gg 1$), one may show using asymptotic forms of the Bessel functions that

$$1/iZ_n \rightarrow \sqrt{\epsilon_1} \cot k_1 \delta \quad (19a)$$

$$iY_n \rightarrow -\sqrt{\epsilon_1} \tan k_1 \delta \quad (19b)$$

(where $k_1 = \omega/c_1 = \sqrt{\epsilon_1} k$, c_1 being the speed of light in the dielectric), and that in the same limit, the right-hand sides of the characteristic equations Eqs. (14) vanish. Accordingly, their solutions are

$$(k_1 \delta)_\ell^{TE} = (2\ell+1)\pi/2 \quad (20a)$$

$$(k_1 \delta)_\ell^{TM} = \ell\pi \quad (20b)$$

with $\ell = \text{integer}$. We therefore have for the spacing of two adjacent (TE or TM) resonances in the high-frequency spectral region (on the k - scale):

$$(k\delta)_{\ell+1}^{TE, TM} - (k\delta)_\ell^{TE, TM} = \pi/\sqrt{\epsilon_1}, \quad (21a)$$

which represents one equation for the two unknowns δ and ϵ_1 of the inverse problem. Calling $\delta = a-b = a(1-\gamma)$, and $\Delta_\ell = x_{\ell+1}^{TE, TM} - x_\ell^{TE, TM}$ the spacing on the x - scale, Eq. (21a) may be written as

$$\sqrt{\epsilon_1} = \frac{\pi}{\Delta_\ell (1-\gamma)}. \quad (21b)$$

A second equation for the unknowns may be found from a consideration of the resonance widths. These are given by the resonance theory in the form (e.g. for TE):

$$\frac{1}{2} \Gamma_{nl}^{TE} = \frac{\text{Im} (z_m^{(2)}(x))^{-1}}{\text{Re} (z_m^{(2)}(x))^{-1} - 1/iZ_n} (x - x_{nl}^{TE}). \quad (22a)$$

When evaluated at one half-width below the resonance, i.e. at $x = x_l^{TE} - \Gamma_l^{TE}/2 \equiv X_l^{TE}$, and using asymptotic forms, one obtains the equation

$$\sqrt{\epsilon_1} = \tan [X_l^{TE} \sqrt{\epsilon_1} (1-\gamma)], \quad (22b)$$

which together with Eq. (21b) suffices to determine the two unknowns ϵ_1 and γ of the problem from the measured resonance spacings Δ_l and resonance widths Γ_l in the high-frequency region of the resonance spectrum.

V. Conclusion

The foregoing discussion has demonstrated on the basis of some selected examples from acoustic, elastic-wave and electromagnetic scattering, that the presence of resonances in scattering cross sections, and their analysis by the resonance theory of scattering as recently developed by us, may serve to solve the inverse scattering problem in a rather direct fashion. For the simple examples considered here, all the unknown material parameters of the target could be obtained from a measurement of the asymptotic spacing and of the width of the resonances. A known shape (flat layers, or spherical objects) has been assumed for the targets of the examples considered. It is clear, however, that the resonance spectrum, and the widths as well as the intensities of the resonance lines, will depend equally well on the geometrical shape as on the material composition of the target (in fact, for impenetrable targets such as acoustically rigid objects or perfect conductors, the spectrum will depend on shape only). A complete experimental determination of the properties of all the resonances appearing in the echo returns from scattering objects should therefore identify the object as far as its geometrical shape and material composition is concerned, in the same fashion in which optical spectra identify chemical substances that emit these spectra. An entire scientific discipline of acoustic, elastic-wave or electromagnetic spectral analysis could therefore be developed for more or less complex scattering objects, with the above-discussed basic examples to be considered as a starting point.

Acknowledgements

The first two authors (G.C.G. and H.Ü.) acknowledge the support of the Independent Research Board of the Naval Surface Weapons Center in the preparation of this work. The second author (H.Ü.) further acknowledges the support of Code 421 of the Office of Naval Research concerning the acoustic work presented here, and the support of AIR-310-B, Naval Air Systems Command, regarding the electromagnetic contribution.

All the authors wish to thank Dr. W. Madigosky, Dr. R. Fiorito, Mr. P. J. Moser and Dr. J. D. Murphy for help and discussions.

References and Footnotes

1. See, e.g., N. Bleistein and N. N. Bojarski, Dept. of Mathematics, Univ. of Denver Report MS-R-7501, 1975.
2. W. G. Neubauer, R. H. Vogt, and L. R. Dragonette, J. Acoust. Soc. Am. 55, 1123 (1974); L. R. Dragonette, R. H. Vogt, L. Flax, and W. G. Neubauer, J. Acoust. Soc. Am. 55, 1130 (1974); H. D. Dardy, J. A. Bucaro, L. S. Scheutz and L. R. Dragonette, J. Acoust. Soc. Am. 62, 1373 (1977).
3. Y. H. Pao and W. Sachse, J. Acoust. Soc. Am. 56, 1478 (1974).
4. See, e.g., G. T. Ruck, D. E. Barrick, W. D. Stuart, and C. K. Krichbaum, Radar Cross Section Handbook, Plenum, New York, 1970.
5. L. Flax, G. C. Gaunaurd, and H. Überall, "Theory of Resonance Scattering", in Physical Acoustics (W. P. Mason and R. N. Thurston, eds.) vol. 15, Academic Press, New York, 1980 (in press).
6. L. Flax, L. R. Dragonette, and H. Überall, J. Acoust. Soc. Am. 63, 723 (1978).
7. G. C. Gaunaurd and H. Überall, J. Acoust. Soc. Am. 63, 1699 (1978)
8. J. D. Murphy, P. J. Moser, A. Nagl, and H. Überall, IEEE Trans. Antennas Propagat. (submitted).
9. One of the few exceptions seems here to be provided by certain electromagnetic-pulse studies: see, e.g., C.W.Chuang and D.L.Moffat, IEEE Trans. Aerosp. Electron.Syst. AES-12, 583(1976); Carl E. Baum, in Transient Electromagnetic Fields(L.B.Felsen,ed.), vol. 10 of "Topics in Applied Physics", Springer-Verlag, Berlin Heidelberg New York 1976; H.Überall and G.C.Gaunaurd, to be published.

10. R. Fiorito and H. Überall, J. Acoust. Soc. Am. 65, 9 (1979).
11. R. Fiorito, W. Madigosky, and H. Überall, J. Acoust. Soc. Am. 66, 1857 (1979).
12. G. C. Gaunaurd, and H. Überall, J. Appl. Phys. 50, 4692(1979).
13. G. C. Gaunaurd and H. Überall, SCIENCE 206, 61 (1979).
14. G. C. Gaunaurd and H. Überall, J. Appl. Mech. 46, 958(1979).
15. G. Gaunaurd, H. Überall, and P. J. Moser, to be published in J. Appl. Physics.
16. P. J. Moser, J. D. Murphy, and H. Überall, to be published in Radio Science.

Figure Captions

- Fig. 1. Plots of $|T|^2$ vs fd at various angles of incidence θ for the exact expression (solid curves), and for the individual resonances in the resonance approximation (broken curves); case of a water layer in alcohol. Primed numbers corresponding to symmetric, unprimed to antisymmetric resonances. Here $\theta_c = 41.8102^\circ$; f = frequency.
- Fig. 2. Transmission loss in decibels versus θ at 73.1 kHz-in.; (top portion): superposition of resonance forms; (bottom portion): calculated from exact theory; for a steel plate in water.
- Fig. 3. Modulus of summed $p \rightarrow p$ backscattered amplitude plotted vs. $k_d a$ (adding 15 terms in the mode series) for an alcohol-filled cavity in aluminum. Some of the rapid oscillations in this plot are accounted for (as indicated) by the resonances shown in the following figure.
- Fig. 4. The zeroth (i.e. $n = 0$) modal contribution (top) of the $|\int p^p / a|$ amplitude of an alcohol-filled spherical cavity in an aluminum matrix, and its separation into a smooth background (center) and isolated resonances (bottom). The resonances in this $n=0$ mode are labeled and marked. The asymptotic spacing is seen to be $\Delta \cong 0.59$.
- Fig. 5. Comparison of theory (solid curve) and experimental observation (points) for the modulus of the far-field acoustic backscattering amplitude of an aluminum cylinder in water.

Fig. 6. Backscattering cross section of a perfectly conducting sphere coated with a lossless dielectric of dielectric constant $\epsilon_1 = 6$, and relative coating thickness $\delta_r = 0.1$, as a function of k_a . Electric (nEl) and magnetic (nMl) resonances are identified by arrows.

Fig. 7. Partial-wave TE- moduli $[(2n+1)/n(n+1)] |a_n|$ plotted vs. ka , for $n = 9$ (top) and 10 (bottom).

Fig. 1

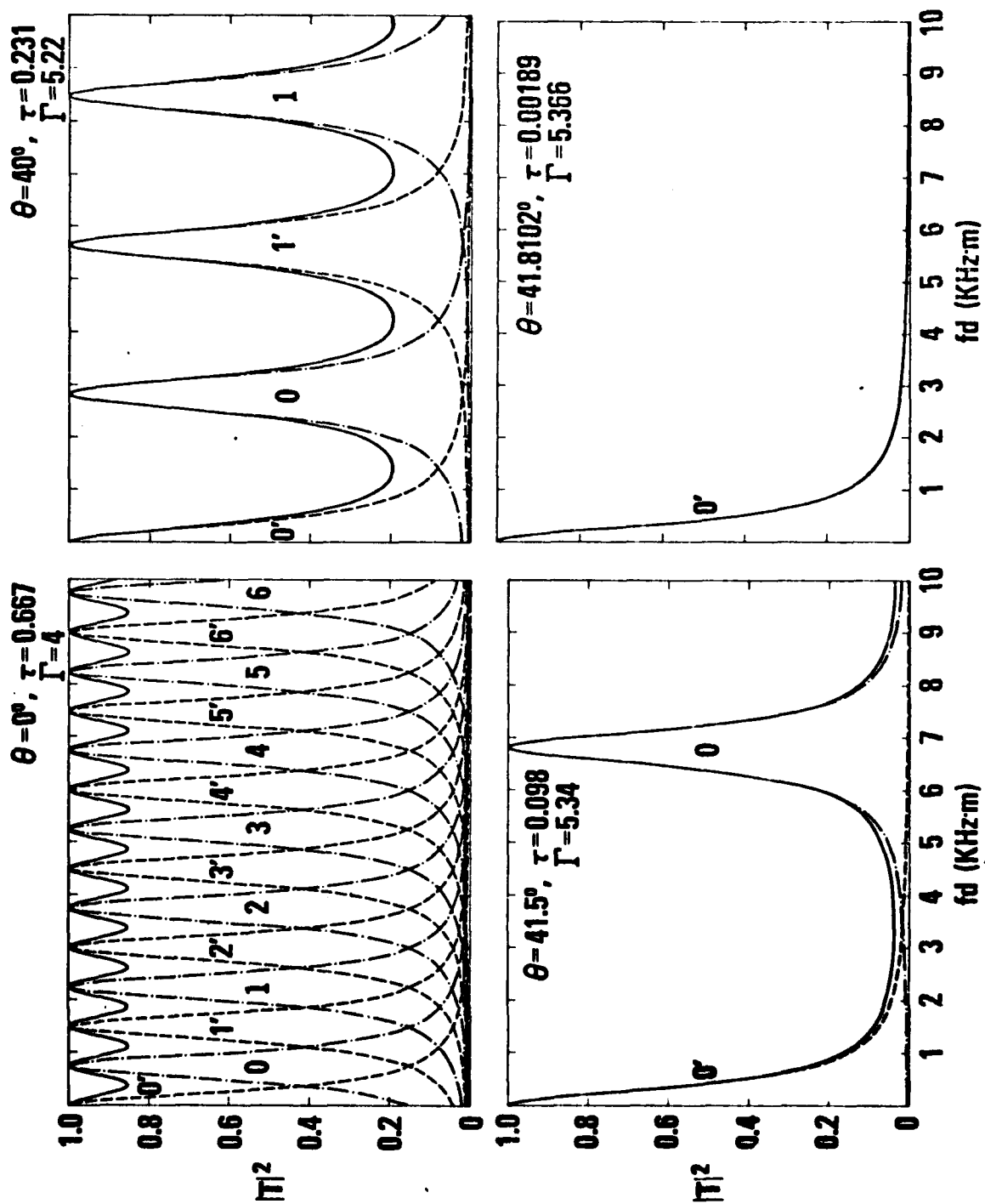


Fig. 2

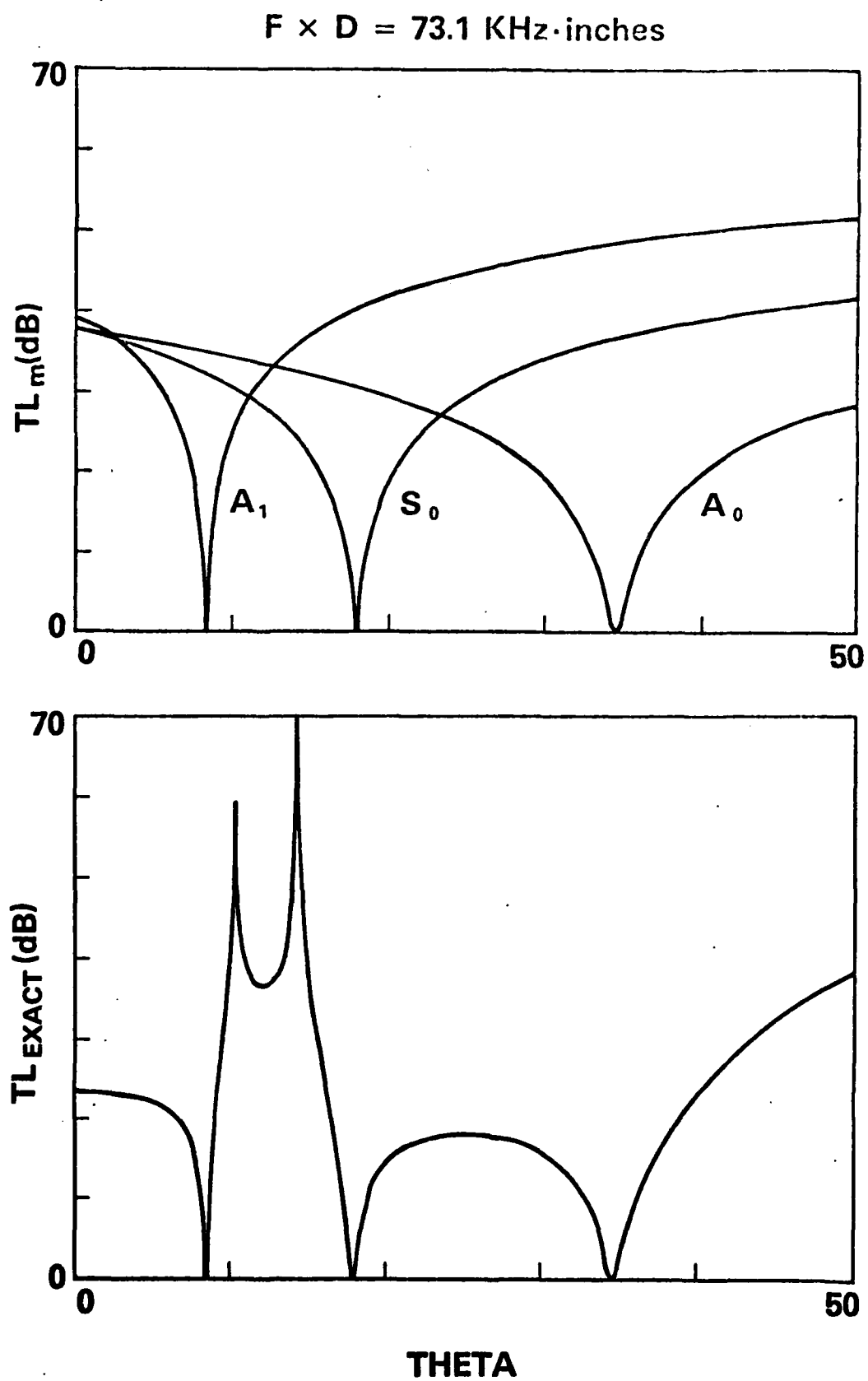


Fig. 2

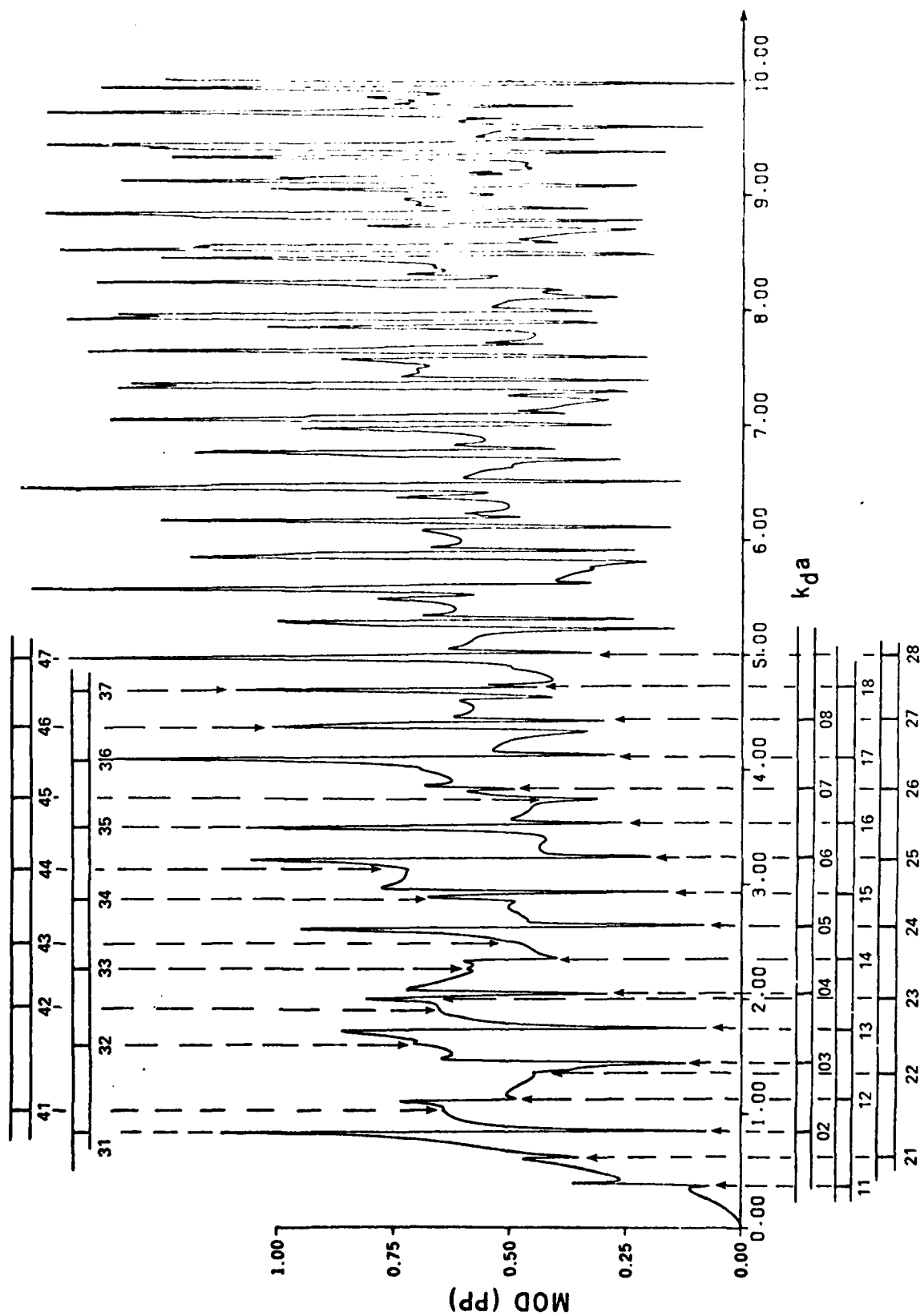
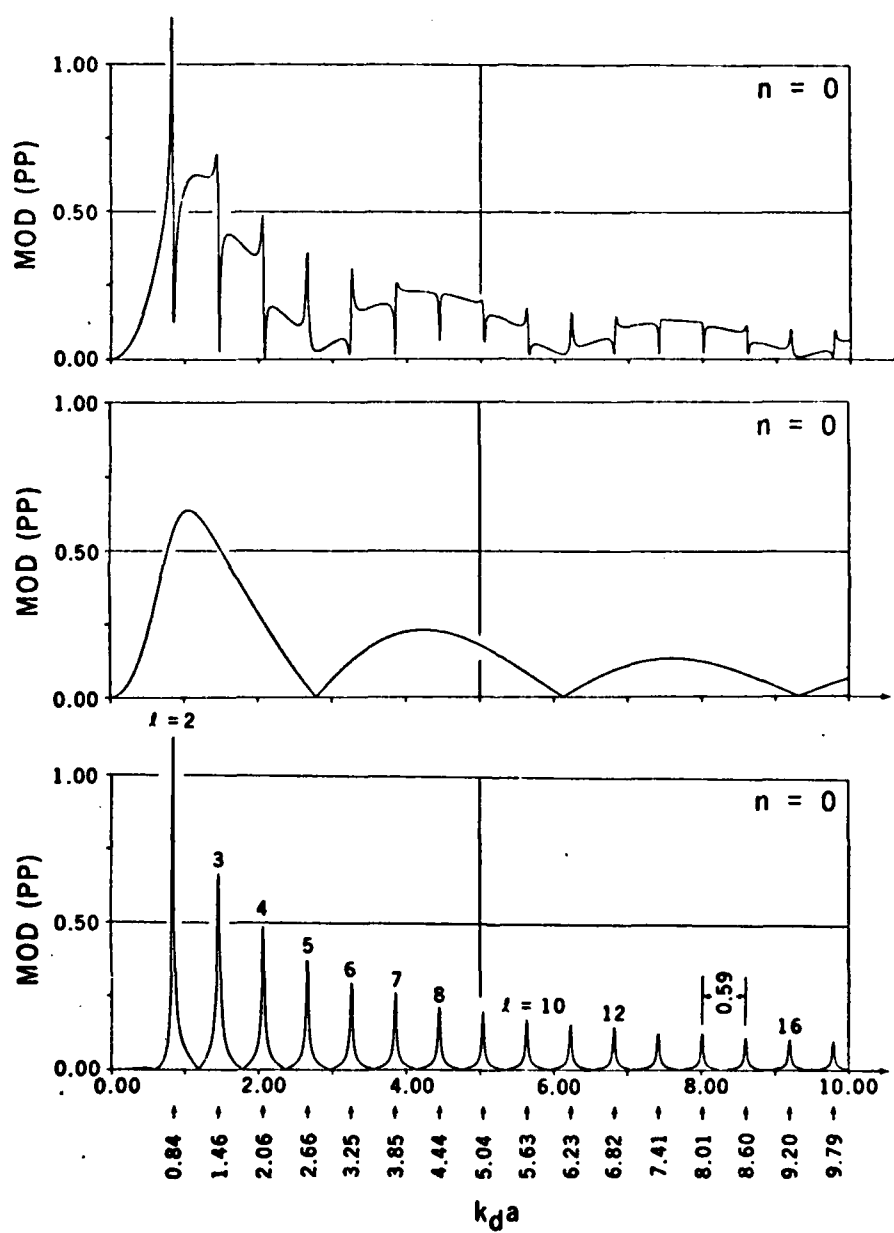


Fig. 4



REFLECTION FROM SOLID ALUMINIUM CYLINDER

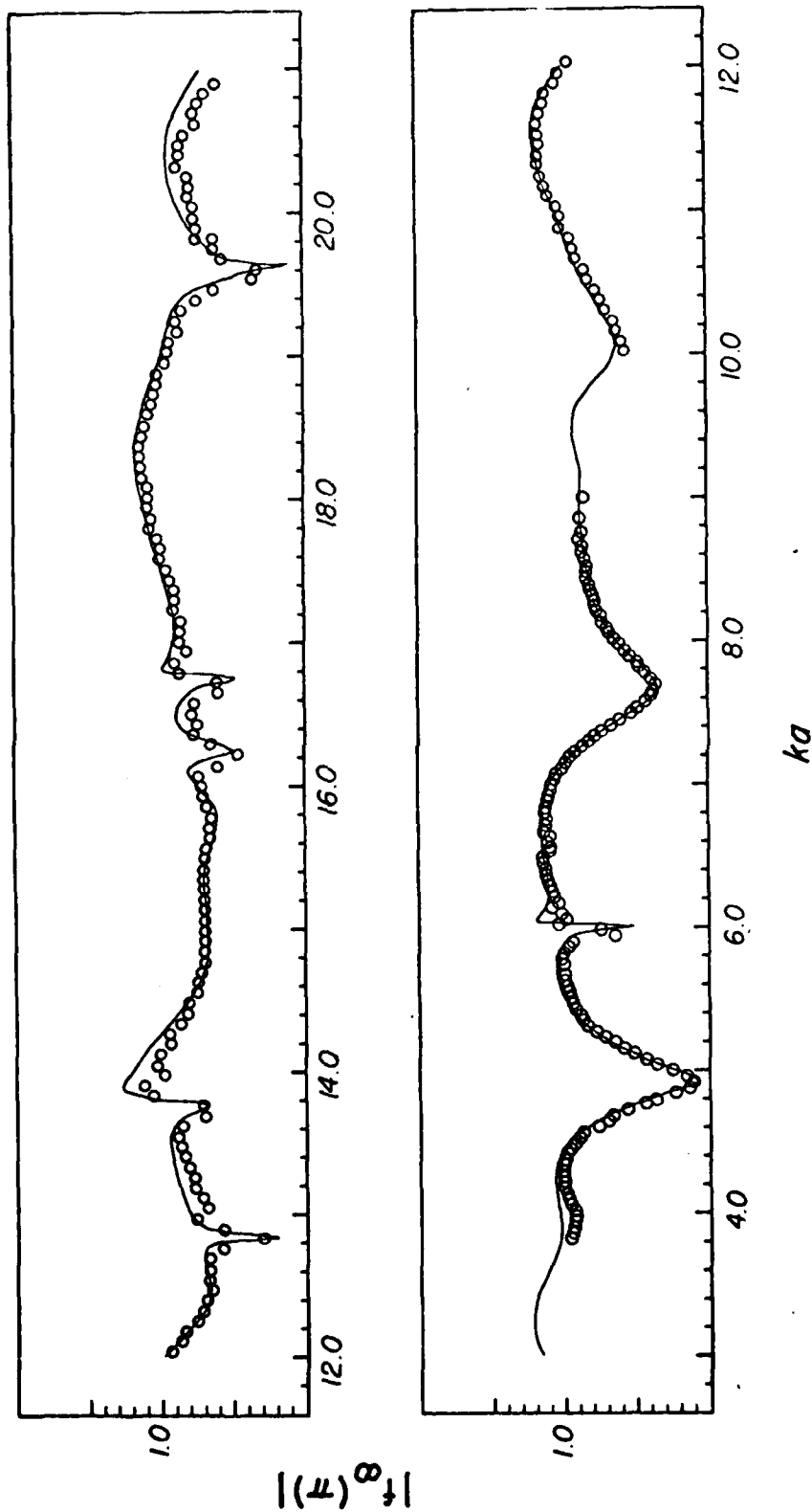


Fig. 5

Fig.6

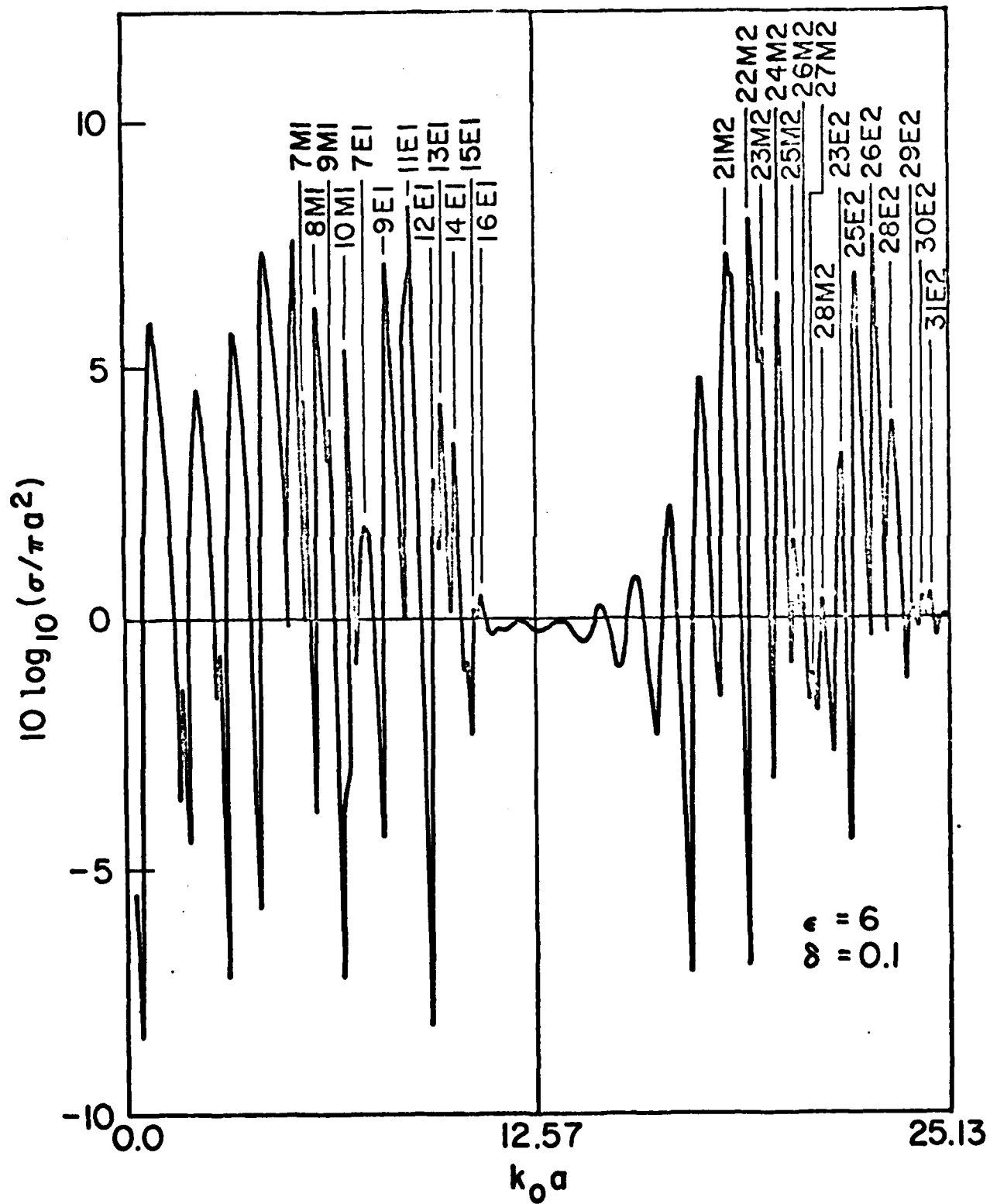


Fig. 7(top)

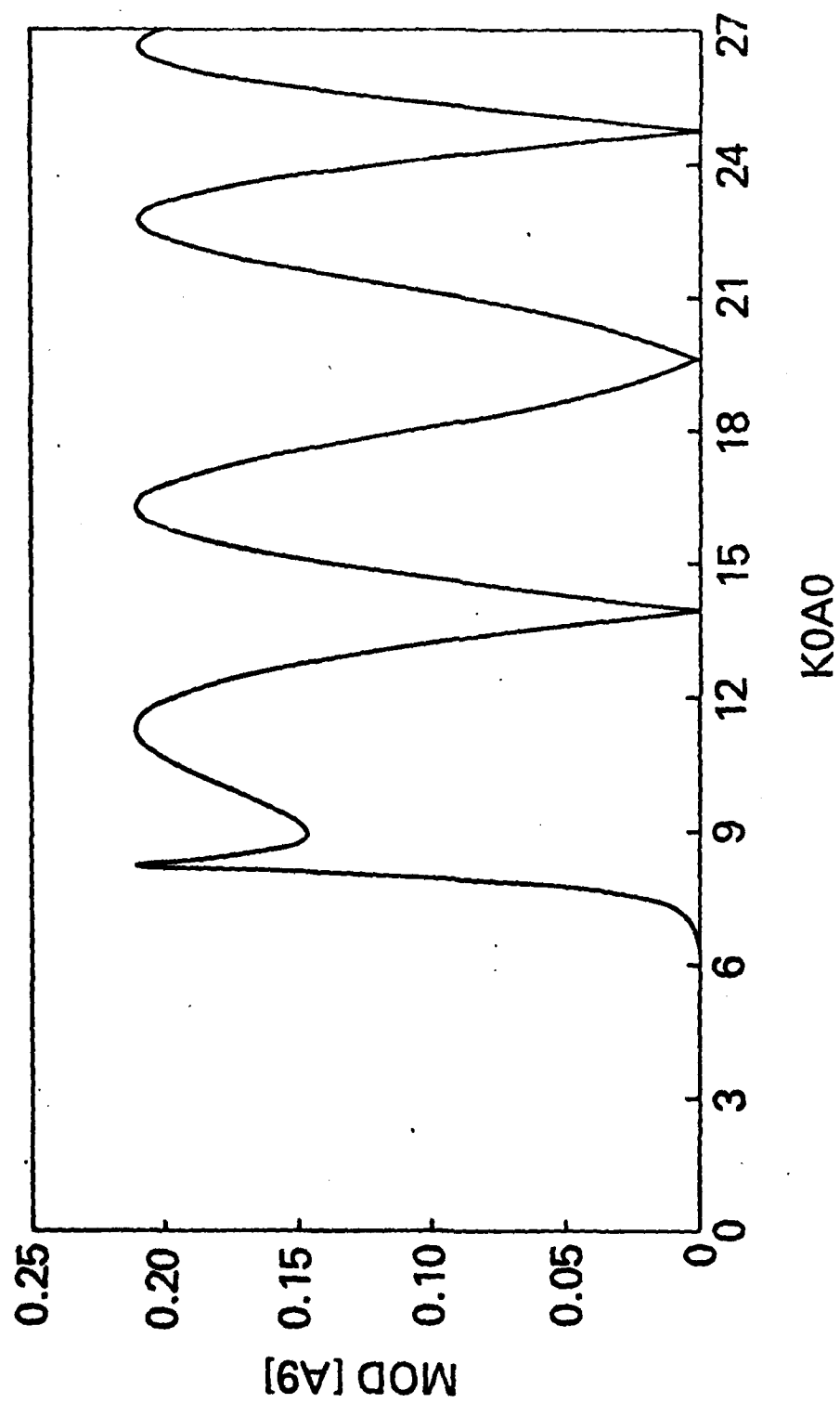


Fig. 7 (bottom)

